Tilt Texture Domains on a Membrane and Chirality Induced Budding

Sarasij R.C.[1] and Madan Rao[1,2]

[1]*Raman Research Institute, C.V. Raman Avenue, Sadashivanagar, Bangalore 560080, India*
[2]*National Centre for Biological Sciences, UAS-GKVK Campus, Bellary Road, Bangalore 560065, India*

We study the equilibrium conformations of a lipid domain on a planar fluid membrane where the domain is decorated by a vector field representing the tilt of the stiff fatty acid chains of the lipid molecules, while the surrounding membrane is fluid and structureless. The inclusion of chirality in the bulk of the domain induces a novel *budding* of the membrane, which *preempts* the budding induced by a decrease in interfacial tension.

The *budding* of membrane vesicles and subsequent *fission* is the only means of traffic between compartmental boundaries within a living cell [1]. Budding of vesicles clearly requires membrane deformation—coat proteins such as Clathrin and COPs I-II have been postulated to play a crucial role in facilitating this deformation. However, the precise role of these coat proteins in budding events remains poorly understood [2].

Membrane deformation leading to budding may also be triggered by changes in the structure and composition of lipids. An oft-quoted mechanism, especially in the context of artificial membranes, is the phase segregation in multicomponent systems which leads to budding due to a decrease in the interfacial energy [3,4] between the lipid components. However, the resulting bud has a radius $R_{bud} > \kappa/2\lambda$, where κ is the bending modulus of the membrane and λ the interfacial tension, which for typical lipids is of order 5 μm, *much too large compared to the budding events in the cell*. In this Letter we propose a novel budding mechanism in a multicomponent lipid membrane, where one of the species is chiral and acquires a tilt. This *chirality-induced budding* can result in a bud size as small as 500 Å.

Consider for simplicity a lipid bilayer membrane, where the upper layer is built of two species, a majority component (e.g., DPPE) and a minority component (e.g., sphingolipid), while the lower layer consists of a uniform density of DPPE [5]. Let the minority species (sphingolipid) acquire a tilt with respect to the local normal of the membrane. The tilt [6] could be intrinsic (when the temperature $T < T_m$, the main transition temperature of the chosen lipid) or acquired due to association with a third component (e.g., cholesterol). We will work in the temperature regime where there is at least a microphase separation of the two lipid components over a length scale R of the order of, say, 1000 Å. Note that most cellular lipids are chiral and so, on acquiring a tilt, this molecular chirality will express itself at length scales much larger than molecular dimensions. The chiral strength may, of course, be enhanced by forming complexes with cholesterol [7].

To start with, let us assume that the sphingolipid complex is spread, with a fixed, uniform density, across a domain of area A, small enough so that over this scale the membrane may be assumed flat. As a result, our description entails a decoration of a planar domain by a two-dimensional (2D) unit vector field **m**, representing the projection of the stiff lipid chains onto the plane of the membrane, while the surrounding membrane is fluid and structureless.

Our low energy Hamiltonian for the membrane tilt domain is given, to quadratic order in the fields by $E = E_B + E_L$ [8], where the bulk energy

$$E_B = \int_A \frac{k_1}{2} (\nabla \cdot \mathbf{m})^2 + \frac{k_2}{2} (\nabla \times \mathbf{m})^2 + k_c (\nabla \cdot \mathbf{m})(\nabla \times \mathbf{m}), \quad (1)$$

and the interfacial energy,

$$E_L = \oint dl[\sigma_0 + \sigma_1(\mathbf{m} \cdot \mathbf{n}) + \sigma_2(\mathbf{m} \times \mathbf{n})]. \quad (2)$$

The unit normal to the boundary **n** aims everywhere into the domain. Note that $\nabla \times \mathbf{m}$ is a pseudoscalar in two dimensions and $k_c(\nabla \cdot \mathbf{m})(\nabla \times \mathbf{m})$ is the bulk chiral contribution to the energy. The magnitude of k_c is set by the density of cholesterol present in the sphingolipid complex. σ_0, the isotropic line tension, is of the order of 10^{-8} dyne. The Frank constants k_1 and k_2 are $\sim 10k_B T_{room}$, while interfacial energy of a domain of radius 0.05 μm is of the same order [9]. This implies that thermal fluctuations can be ignored at the temperatures of interest. We set $k_1 = 1$ as our unit of energy and $\sigma_0 = 1$ as our unit of length (equivalent to a length of order 0.1 μm).

The Hamiltonian (1), (2) has been studied in [8,10] in the context of textures on Sm-C* films and Langmuir monolayers, respectively. Apart from the context, there are three major points of departure—(i) our variational calculation and Monte Carlo (MC) simulations for the $T = 0$ phase diagram are "exact" giving results very different from [10], (ii) we study the effect of strong anisotropic line tension and bulk chirality on the shape and texture of the domain, and (iii) we couple the tilt field to the local curvature of the

membrane and study the effect of chirality on membrane shape.

We rotate our coordinate axes and redefine the coefficient of anisotropic line tension to obtain the simpler expression [8,10] $E_L = \oint dl[\sigma_0 + \sigma(\mathbf{m} \cdot \mathbf{n})]$. The $T = 0$ phase diagram is obtained by minimizing E variationally subject to the constant area A constraint. Our variational ansatz is restricted to a connected domain and so does not allow for the breakup of domains into multiple domains. In all cases, we have corroborated the results of our variational calculation by an MC simulation using simulated annealing to avoid getting stuck in local minima. In this sense our variational calculation is exact.

We first study the phase diagram of a domain with circular boundaries. To begin with, let us turn off bulk chirality ($k_c = 0$) and set $k_2 = k_1$. The $T = 0$ phase diagram in the R-σ plane (where $R = \sqrt{A/\pi}$) has the following four phases separated by first-order boundaries (Fig. 1): (1) *Boojum* phase where the center of the circular domain is a distance a away from the core of a virtual defect of strength N. Placing the origin of polar coordinates (r, θ) at the core of the boojum, we can describe the texture $\mathbf{m} \equiv (\cos\phi, \sin\phi)$ by the equation

$$\phi = N\theta + c_1 r \sin\theta + c_2 r^2 \sin2\theta + c_3 r^3 \sin3\theta + \dots . \tag{3}$$

The energy E is minimized with respect to the variational parameters $(N, a, \{c_n\})$ for fixed (R, σ). We find that the optimal value of N is exactly 2, independent of a. In drawing the phase diagram we parametrize the texture by N and c_1 alone; inclusion of c_2 and terms of higher order lowers the energy by 1% at most. Fixing the area at, say, $R = 1$, an increase in σ leads to an increase in c_1 and pushes the core of the virtual defect towards the domain center, till at $a = 1.7$ we enter the annular phase. (2) *Achiral*
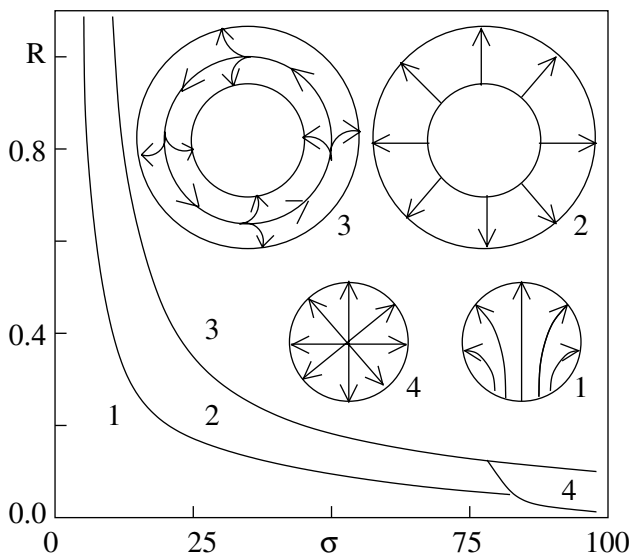
FIG. 1. Phases of the tilt texture domain with circular periphery: (1) Boojum, (2) achiral annular, (3) chiral annular, and (4) hedgehog with $\epsilon_c = 0$. Arrows indicate direction of $\mathbf{m}$ field.

annular phase with inner and outer radii r_1 and r_2, respectively. At the outer rim of the annulus $\mathbf{m}$ is directed radially outward, while at the inner boundary $\mathbf{m}$ is inclined at an angle α to the local normal $\mathbf{n}$. With the origin of polar coordinates at the center of the annulus, the texture may be described by $\phi = \theta - \alpha(r_2 - r)/(r_2 - r_1)$, where r_1, α are variational parameters. The inner radius r_1 monotonically decreases as we increase σ such that $\mathbf{m}$ always points radially outward ($\alpha = 0$) at every point of the domain. As one crosses the first-order phase boundary (Fig. 1) we encounter a new annular phase with a chiral texture. (3) *Chiral annular* phase where α jumps to an angle greater than $\pi/2$ at both boundaries. Consequently, the bulk texture is chiral with the order parameter $C = \int d^2x (\nabla \cdot \mathbf{m})(\nabla \times \mathbf{m}) \neq 0$ *even though there is no bulk chiral interaction*. This chiral phase is doubly degenerate and can spontaneously acquire either sign. (4) *Hedgehog* phase with a defect at the domain center and a texture described by $\phi = \theta$. The energy includes a core contribution ϵ_c of the defect of size r_c.

The transitions $1 \rightarrow 2$ and $2 \rightarrow 3$ are discontinuous (indicated by the change in slope of the energy branches as a function of σ) and weaken as the domain size R shrinks.

As σ_0 is reduced, the boundary of the domain is no longer constrained to be circular. We may then parametrize the boundary by smooth deformations of a circle, $r(\theta)$, where the origin is at the center of the circle of radius r_0 and $0 < \theta < 2\pi$ is the angle to the polar axis, $r(\theta) = r_0[1 + \sum_{n=1}^{\infty} \alpha_n \cos(n\theta)]$. The amplitudes $\{\alpha_n\}$ are additional parameters in our variational calculation. We find that the texture throughout the R-σ plane is a boojum with the domain bulging out near the equator and flattening near the poles as σ increases from zero. These shapes and textures win over the annular and hedgehog phases.

We now turn to a description of phases with nonzero bulk chirality k_c, which without loss of generality we take to be positive. In the phase diagram, Fig. 2, we have set $\sigma = 0$: (1) *Uniform* phase, when $|k_c| < 1$, where the domain is circular and the tilt field $\mathbf{m}$ is uniform. (2) *Spiral hedgehog* phase where the domain is circular with a texture such that $\mathbf{m}$ at every point is inclined at an angle α to the ray emanating from the center of the domain. The radial and the tangential components of $\mathbf{m}$ in this spiral phase are $m_r = \cos\alpha$, $m_\theta = \sin\alpha$, while the energy is given by

$$E = 2\pi(r_c + R) - \left(\frac{k_c}{2}\sin2\alpha - \frac{1}{2}\right)\log\frac{R}{r_c} + \epsilon_c . \tag{4}$$

The optimum value of α is $\pi/4$ when $|k_c| > 1$. This phase clearly gives a nonzero value for the chiral order parameter C. (3) *Tweed* phase domain is again circular though the texture loses the circular symmetry of the previous phase. Our ansatz for the texture is motivated by the results of an MC simulation of 3055 particles carrying O(2) spins on a triangular lattice with a Hamiltonian obtained by discretizing E, for $\sigma = 0$, $k_c = 12.75$. We have performed a
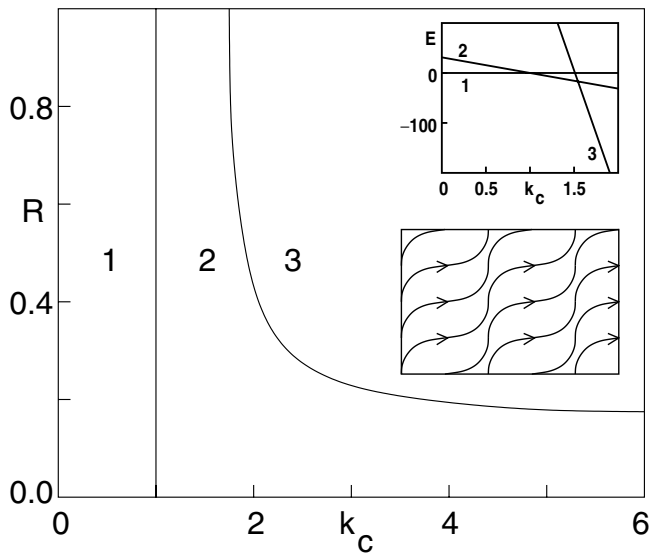
FIG. 2. Phases of the tilt texture domain with bulk chirality and $\sigma = 0$: (1) Uniform, (2) spiral hedgehog ($\epsilon_c = 0$), and (3) tweed. Top inset shows variation of the energy branches as a function of k_c at $R = 1$ indicating discontinuous transitions. Notice that the energy decreases rapidly in phase (3) as k_c increases. Lower inset shows the texture within a unit cell; this pattern repeats periodically to form the tweed phase (3).

simulated annealing from $(k_B T)^{-1} = 0.1 \rightarrow 300$ starting from a variety of initial conditions [11] to obtain textures as in Fig. 2 (lower inset). A variational ansatz may easily be written down for such a texture: place the origin of coordinates on the boundary of the domain and parametrize the texture by a length, l, such that $m_x = |\cos x/l|$ and $m_y = -|\sin x/l|$. This texture confers a net chiral strength to the domain—$(\nabla \cdot \mathbf{m})(\nabla \times \mathbf{m})$ has the same sign everywhere, though the sign of individual terms, $\nabla \cdot \mathbf{m}$ and $\nabla \times \mathbf{m}$, varies from one stripe to the next. The energy of the tweed domain is

$$E = 2\pi R - \frac{k_c}{2l^2} \int_0^{2R} dx \sqrt{2xR - x^2} \left| \sin \frac{2x}{l} \right| + \frac{1}{2l^2}. \tag{5}$$

The variational parameter l approaches zero to minimize the energy, corresponding to infinitely many tweeds. Higher order derivative terms in the Hamiltonian would, however, cut off this monotonic decrease at some scale l^* [11].

On turning on the anisotropic line tension σ, the boundary of the domain deviates from a circle giving rise to a variety of new phases. We will make a detailed study of the phase diagram in a later paper. Let us move on, for the moment, and allow the membrane containing the domain to be flexible, thus promoting a coupling between the tilt field $\mathbf{m}$ and the curvature tensor K_{ij} [12]. At the same time we have to treat the membrane as a bilayer: we thus define the curvature, tilt, and lipid density fields on both the upper and lower leaves of the bilayer and project these variables onto the neutral surface of the membrane [13]. In covari-

ant form, the bulk energy to lowest order in derivatives is given by [14]

$$E_B = \int_A \left[\frac{k_1}{2} (\mathrm{div}\mathbf{m})^2 + \frac{k_2}{2} (\mathrm{curl}\mathbf{m})^2 \right.$$
$$+ k_c (\mathrm{div}\mathbf{m})(\mathrm{curl}\mathbf{m}) + c_0 K_i^i + \frac{\kappa}{2} (K_i^i)^2$$
$$\left. + \beta m^i m^j K_j^i + c_0^* \gamma_{ij} m^k m^i K_k^j \right], \tag{6}$$

where the divergence and curl are written in terms of the covariant derivative D_i as, $\mathrm{div}\mathbf{m} = D_i m^i$ and $\mathrm{curl}\mathbf{m} = \gamma_i^j D_j m^i$. The terms proportional to c_0 and κ are the usual Helfrich contributions to the membrane energy [15]. The appearance of γ_{ij}, the completely antisymmetric tensor on a 2D curved manifold [12], indicates that the coupling of the texture to the membrane curvature also depends on the chiral strength of the sphingolipid complex [7] in the domain. The magnitude of this term is proportional to the curvature of the membrane if the texture on the membrane has a handedness; this favors a helical texture on a cylindrical membrane, the lines of $\vec{m}$ being inclined at an angle of 45° to the axis of the cylinder. To highlight the effect of chirality, we set $c_0 = \beta = 0$ and include only the isotropic line tension in the interfacial energy E_L [16].

We will see that the effect of increasing c_0^* for fixed size R is to induce the domain to leave the plane and form a spherical bud of radius $R/2$ connected to the plane by an infinitesimal neck. More significantly, at fixed but large enough c_0^* this *chirality induced budding occurs at a much smaller size R than the phase separation induced budding caused by a decrease in the interfacial tension between the two lipid components* [3]. Note that we have ignored higher order derivative terms in (6) which couple gradients of $\vec{m}$ to the curvature; we have seen that its effect is small, merely renormalizing the spontaneous curvature.

For instance if we fix k_c at phase (2) of Fig. 2, we find that the membrane remains *planar* and the texture a spiral hedgehog for small c_0^* (Fig. 3). A further increase in c_0^* leads to a discontinuous budding transition where the texture decorates a spherical bud with a vanishingly thin neck. Both the chiral terms, proportional to k_c and c_0^*, gain in energy by this budding, even at the cost of producing a defect at the pole. This may be seen by setting the latitudinal and longitudinal components of $\mathbf{m}$ as $m_\theta = 1/\sqrt{2}$ and $m_\phi = 1/\sqrt{2}$, a choice which smoothly goes over to the spiral hedgehog phase in the limit of the planar membrane. The membrane shape is parametrized as a sphere of radius r attached to the plane by a neck of radius r_0. The energy of this conformation is $E_L = 2\pi r_0$ and

$$E_B = \pi\kappa \frac{R^2}{2r^2} - \pi c_0^* \frac{R^2}{r}$$
$$- \pi(k_c - 1) \int_{\theta_c}^{\pi-\theta_0} d\theta \frac{\cos^2\theta}{\sin\theta}, \tag{7}$$

in addition to a defect core energy ϵ_c, where $\theta_c = r_c/r$ and $r_0 = r \sin\theta_0$. As before, we have fixed our unit of energy by setting $k_1 = k_2 = 1$. We have ignored the small
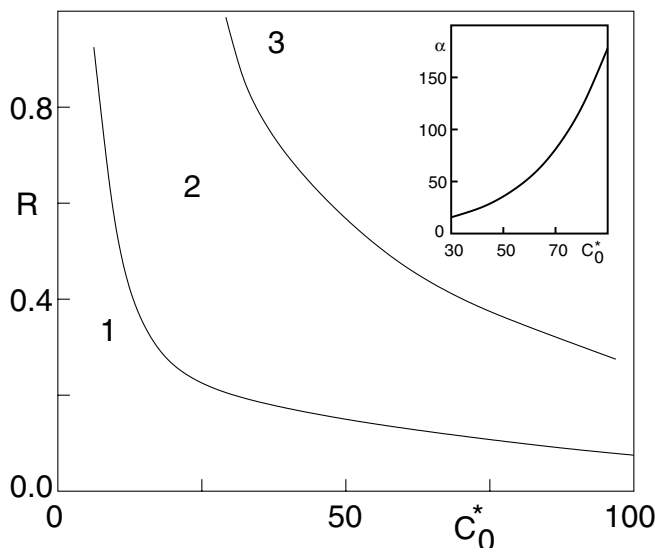
FIG. 3. Phases of the tilt domain coupled to membrane shape with $k_c = 1.5$, $\sigma = 0$, and $\kappa = 10$: (1) Planar, (2) spherical bud, and (3) cylindrical tubule. With these parameters, domain induced budding due to a gain in line tension [3] occurs at $R_c = 10$. Inset shows the variation of the ratio $\alpha = L/r$ with c_0^* for a domain of size $R = 1$.

curvature energy cost at the junction where the spherical bud meets the plane. Variation suggests that the energy is minimized when $r_0 \rightarrow 0$ and $r = R/2$ (Fig. 3).

At larger values of c_0^*, the spherical bud gives way discontinuously to a *cylindrical tubule* (Fig. 3). We see that the energy is minimized when the domain wraps around a cylinder of radius r and length L attached to the plane at one end and capped by a hemisphere with a polar defect core at the other (Fig. 3). The **m** field on the spherical cap is as described earlier; the axial and tangential components of **m** on the cylinder are $m_z = 1/\sqrt{2}$ and $m_\phi = 1/\sqrt{2}$. This choice corresponds to a texture where the lines of **m** wrap around the cylinder as a helix of pitch proportional to r [17]. Note that **m** varies smoothly across the junction of the cylinder and the hemisphere, and extrapolates smoothly to the spiral hedgehog texture in the limit of the planar membrane. The energy of this conformation is $E_L = 2\pi r$ and

$$E_B = 2\pi\left(\frac{\kappa}{2} - c_0^* r\right) + \pi\left(\frac{\kappa}{4} - c_0^* r\right)\left(\frac{R^2}{2r^2} - 1\right)$$
$$- \pi(k_c - 1)\int_{\theta_c}^{\pi-\theta_0} d\theta\, \frac{\cos^2\theta}{\sin\theta}, \qquad (8)$$

in addition to a core energy ϵ_c (we have again ignored the curvature contribution coming from the neck). The optimal L/r obtained variationally increases rapidly with c_0^* [Fig. 3 (inset)].

As seen from the inset of Fig. 2, the energy plummets as k_c increases. This implies that if k_c was chosen such that

phase (3) of Fig. 2 were the equilibrium texture at $c_0^* = 0$, then the domain would gain significantly in bulk energy by budding, first into a spherical bud and then into a tubule. The range of c_0^* for which the spherical bud obtains would, however, be reduced.

The variational calculation for the energy-minimizing shapes of a flexible, fluid membrane having a tilt domain is, of course, not exact. A more general variational calculation will at most shift the phase boundaries slightly; in any case, the *chirality-induced budding* at small R is robust and should be testable in experiments on artificial membranes consisting of carefully chosen lipid components. We believe that this is relevant to the budding of cell membranes which are not assisted by coat proteins, as in the endocytosis of raft components [18].

[1] B. Alberts *et al., Molecular Biology of the Cell* (Garland Publishing, New York, 1994), 3rd ed.

[2] R. Nossal, Traffic **2**, 138 (2001).

[3] R. Lipowsky, Biophys. J. **64**, 1133 (1993).

[4] H. Döbereiner *et al.,* Biophys. J. **65**, 1396 (1993).

[5] This picture is inspired by recent discussions on membrane "rafts" in K. Simmons and E. Ikonen, Nature (London) **387**, 569 (1997); T. Harder and K. Simmons, Curr. Opin. Cell Biol. **9**, 534 (1997); M. Edidin, Curr. Opin. Struct. Biol. **7**, 528 (1997).

[6] J. Israelachvili, *Intermolecular and Surface Forces* (Academic Press, London, 1998).

[7] A. Radhakrishnan, T. Anderson, and H. McConnell, Proc. Natl. Acad. Sci. U.S.A. **97**, 12 422 (2000).

[8] S. Langer and J. Sethna, Phys. Rev. A **34**, 5035 (1986).

[9] The dipole-dipole interaction energy per lipid is about 10^{-15} erg, 2 orders smaller than the Frank energy (1) and hence may be ignored.

[10] D. Pettey and T. Lubensky, Phys. Rev. E **59**, 1834 (1999).

[11] A higher order term $\gamma[(\text{div}\mathbf{m})^4 + (\text{curl}\mathbf{m})^4]$ in the MC simulation provides a cutoff to the stripe size.

[12] W. Helfrich and J. Prost, Phys. Rev. A **38**, 3065 (1988).

[13] U. Seifert, J. Shillcock, and P. Nelson, Phys. Rev. Lett. **77**, 5237 (1994).

[14] P. Nelson and T. Powers, Phys. Rev. Lett. **69**, 3409 (1992).

[15] W. Helfrich, Z. Naturforsch. C **28**, 693 (1973).

[16] Inclusion of c_0 and β would merely favor the budding transition owing to the intrinsic asymmetry of the bilayer.

[17] J. V. Selinger and J. M. Schnur, Phys. Rev. Lett. **71**, 4091 (1993); J. V. Selinger, F. C. Mackintosh, and J. M. Schnur, Phys. Rev. E **53**, 3804 (1996).

[18] C. Lamaze *et al.,* Mol. Cell **7**, 661 (2001); S. Sabharanjak and S. Mayor, Mol. Biol. Cell **10**, 399a (1999).